Phytochemistry 71 (2010) 70–80

Contents lists available at ScienceDirect

Phytochemistry

journal homepage: www.elsevier.com/locate/phytochem

Metabolic profiles of sunflower genotypes with contrasting response to *Sclerotinia sclerotiorum* infection

Lucila Peluffo [a,b], Verónica Lia [a,b,c], Carolina Troglia [d], Carla Maringolo [d], Paniego Norma [a,b], Alberto Escande [d], H. Esteban Hopp [a,c], Anna Lytovchenko [e], Alisdair R. Fernie [e], Ruth Heinz [a,b,c,*], Fernando Carrari [a,b,*,1]

[a] *Instituto de Biotecnología, CICVyA, Instituto Nacional de Tecnología Agropecuaria (IB-INTA), Argentina*
[b] *Consejo Nacional de Investigaciones Científicas y Técnicas (CONICET), Argentina*
[c] *Facultad de Ciencias Exactas y Naturales, Universidad de Buenos Aires, Argentina*
[d] *Unidad integrada INTA Balcarce–Universidad Nacional de Mar del Plata, Argentina*
[e] *Max-Planck-Institut für Molekulare Pflanzenphysiologie, Am Mühlenberg 1, 14476 Postdam-Golm, Germany*

ARTICLE INFO

Article history:
Received 21 January 2009
Received in revised form 23 July 2009
Available online 21 October 2009

Keywords:
Sunflower
Helianthus annuus L.
Compositae
Head rot disease
Metabolite profiling
Sink organ metabolism

ABSTRACT

We report a comprehensive primary metabolite profiling of sunflower (*Helianthus annuus*) genotypes displaying contrasting behavior to *Sclerotinia sclerotiorum* infection. Applying a GC–MS-based metabolite profiling approach, we were able to identify differential patterns involving a total of 63 metabolites including major and minor sugars and sugar alcohols, organic acids, amino acids, fatty acids and few soluble secondary metabolites in the sunflower *capitulum*, the main target organ of pathogen attack. Metabolic changes and disease incidence of the two contrasting genotypes were determined throughout the main infection period (R5.2–R6). Both point-by-point and non-parametric statistical analyses showed metabolic differences between genotypes as well as interaction effects between genotype and time after inoculation. Network correlation analyses suggested that these metabolic changes were synchronized in a time-dependent manner in response to the pathogen. Concerted differential metabolic changes were detected to a higher extent in the susceptible, rather than the resistant genotype, thereby allowing differentiation of modules composed by intermediates of the same pathway which are highly interconnected in the susceptible line but not in the resistant one. Evaluation of these data also demonstrated a genotype specific regulation of distinct metabolic pathways, suggesting the importance of detection of metabolic patterns rather than specific metabolite changes when looking for metabolic markers differentially responding to pathogen infection. In summary, the GC–MS strategy developed in this study was suitable for detection of differences in carbon primary metabolism in sunflower *capitulum*, a tissue which is the main entry point for this and other pathogens which cause great detrimental impact on crop yield.

1. Introduction

Sunflower (*Helianthus annuus* L.) is the third most important source of edible vegetable oil and is additionally anticipated to shortly become an efficient source of biodiesel (Sunflower Statistics, NSA 2007, USA). Moreover, sunflower seeds are an important source of minerals, vitamins, and antioxidants in human food and animal feed, with by-products of oil extraction being of substantial use to the pellet industry (Senkoylu and Dale, 2006).

Pathogen infections not only represent one of the main constraints on productivity, but also have a detrimental impact on quality components of harvestable plant products. *Sclerotinia sclerotiorum* (Lib) de Bary is a worldwide distributed necrotrophic pathogen, differentially attacking more than 400 plant species by inducing diverse symptoms in leaves, stalks and flowers, with head white rot being the most damaging for sunflower crop production (Boland and Hall, 1994; Mestries et al., 1998). Sunflower head rot is an endemic disease in the south–east area of Buenos Aires, Argentina, causing average yield reductions of 10–20% and can even, if the environmental conditions allow, result in loss of the entire harvest (Pereyra and Escande, 1994). *S. sclerotiorum* attacks are difficult to control since there are no efficient chemical treatments for this pathogen. It additionally persists in soils for long periods and is consequently often abundant at high inoculum levels. Moreover, the polygenic character of natural resistance to *S. sclerotiorum* infection means that complete resistance has not been accomplished in

* Corresponding authors. Address: Instituto de Biotecnología, CICV-INTA, CC 25, B1712WAA Castelar – Buenos Aires, Argentina. Tel.: +54 (11) 4621 1447x1676; fax: +54 (11) 4621 0199.
E-mail addresses: rheinz@cnia.inta.gov.ar (R. Heinz), fcarrari@cnia.inta.gov.ar (F. Carrari).
[1] Partner group of the Max Planck Institut für Molekulare Pflanzenphysiologie.

0031-9422/$ - see front matter © 2009 Elsevier Ltd. All rights reserved.
doi:10.1016/j.phytochem.2009.09.018

cultivated sunflower (Rodríguez et al., 2004; Rönicke et al., 2005). Oxalate has been reported as a major pathogenic factor in *S. sclerotiorum* infections (Godoy et al., 1990), being postulated to aid infection via acidification-facilitated cell-wall degradation, pH-mediated tissue damage or Ca^{2+} ion sequestration-mediated cell-wall weakening (for review see Dutton and Evans, 1996). Additionally, oxalate can directly suppress the oxidative burst associated with pathogen detection and activate programmed cell death (Cessna et al., 2000; Kim et al., 2008). That said, plant defense responses to *S. sclerotiorum* attack clearly involve further mechanisms including anatomical defense, pre-formed anti-fungal components, and post-infection anti-fungal compounds (Rodríguez et al., 2004). Moreover, a higher content of phenolic compounds, such as coumarins and chromene, as well as increased phenylalanine ammonia-lyase activity have previously been reported to be present in tolerant in comparison with susceptible genotypes of sunflower (Prats et al., 2003, 2006, 2007).

Germin and germin-like proteins together with oxalate oxidase/superoxide dismutase activity have additionally been associated with defense mechanisms to *S. sclerotiorum* infections in several different species including sunflower (see for example Carter and Thornburg, 2000; Christensen et al., 2004; Dumas et al., 1993; Godfrey et al., 2007; Hu et al., 2003).

As mentioned above, resistance to *S. sclerotiorum* has been characterized as a complex characteristic with different quantitative trait loci (QTL) detected in specific genotypes, plant organs and growth conditions (Gentzbittel et al., 1998; Mestries et al., 1998). Recent studies have identified several QTL associated with *S. sclerotiorum* resistance in sunflower leaves, mid-stalk or *capitula* (Bert et al., 2002, 2004; Micic et al., 2004, 2005a,b). In addition, we have recently developed an integrated genetic map (Kiani et al., 2007; Paniego et al., 2006) that allows facile cross-reference between two previously developed maps (Al-Chaarani et al., 2002, 2004; Tang et al., 2002) and is, therefore, a useful tool in the evaluation of the co-localized QTL. Despite these detailed genetic studies, as yet reports investigating the association of resistance QTL to transcriptional and metabolic changes induced during the sunflower–*S. sclerotiorum* interaction are still scarce. Indeed to our knowledge they are limited to just one – the study of a protein kinase-like locus associated to a single QTL region (Gentzbittel et al., 1998). Moreover, only few studies have reported transcriptional and metabolic analysis of *Sclerotinia* infection. A recent gene expression analysis of the *Brassica napus* response to *S. sclerotiorum*, however, revealed differential expression between resistant and susceptible genotypes for genes associated with jasmonate and ethylene signal transduction pathways as well as WRKY transcriptional factors, plant cell wall related proteins and sugar transporters (Zhao et al., 2007). Studies of soluble metabolite exchange between sunflower and *Sclerotinia* have been performed by Jobic et al. (2007). In addition, changes in sucrose, glucose, glucose 6-phosphate, adenosine and linolenic acid accompanied dramatic changes in benzylisoquinoline alkaloids following elicitor treatment of poppy cell cultures (Zulak et al., 2007). These observations alongside those indicating an effect of pathogen infection on the rate of photosynthesis (Chou et al., 2000; Tang et al., 1996) and carbon partitioning (Depuydt et al., 2009; Abood and Lösel, 2003; Hall and Williams, 2000), suggest an important role for carbon metabolism in aiding in tolerance of plants to pathogens.

A fuller comprehension of the metabolic crosstalk involved in host–pathogen interaction is of importance at both fundamental and applied levels. However, the application of broad metabolite profiling approaches to aid in greater understanding of this process are, as yet, lacking, particularly when target pathogen-infected tissues represent sink organs such as flowers. For this reason, we here adopt a gas chromatography–mass spectrometry (GC–MS)-based metabolite profiling approach capable of identifying a broad spectrum of metabolites including major and minor sugars and sugar alcohols, organic acids, amino acids, fatty acids and few soluble secondary metabolites in the sunflower *capitulum*. This approach has recently proven to be one of the key tools in metabolomics *per se* and by extension in plant functional genomics (for review see: Sumner et al., 2003; Fernie, 2007). As plant–host interactions represent one of the most complex systems at the biochemical level, our aim was to develop a metabolomic approach to shed light onto the metabolism of sunflower florets by a comparative analysis of two well characterized genotypes with contrasting tolerance levels to *S. sclerotiorum*. Metabolite profiling data obtained here show that, under field conditions, primary metabolism is differentially synchronized in these genotypes. Parametric and non-parametric data analyses allowed the identification of a combined effect of several metabolite patterns implicated in the tolerance to this disease.

2. Results

2.1. Experimental design

The experimental system used in the present study consisted of two sunflower inbred lines displaying different tolerance to *S. sclerotiorum* infection: RHA801 (resistant) and HA89 (susceptible). Under controlled cultivation conditions (see Section 5 for details), the crop was inoculated at the R5.2 developmental stage (Fig. 1A) which is the period of maximum susceptibility of sunflower to *S. sclerotiorum* infection in the cultivation areas of South America (latitude 37° 45′ S, longitude 58° 18′ W) (Pereyra and Escande, 1994). In previous work, we demonstrated that the severity index of the disease, based on the proportion of healthy *capitulum* tissue to that of diseased tissue, was significantly different between the two lines (Maringolo, 2007). In the experimental system described herein, the disease incidence (number of plants with symptoms/total number plants) was recorded from 21 to 42 DAI (days after inoculum) and as Area under the Disease Progress Curve (AUDPC) calculated values (Campbell and Madden, 1990) (Fig. 1B). In agreement with previous results, this analysis showed significant differences between the cumulative AUDPC of the evaluated genotypes; 2.36 for RHA 801 and 5.83 for HA 89. Minimum significant differences were 2.76 for AUDPC as resulted by a Waller–Duncan test.

Visual symptoms were not observed until 21 DAI when flower necrosis followed by light tan spots and humid-soft rots of the receptacle took place. Later, as these lesions aged (on average at 43 DAI), the *capitula* became bleached and shredded with only vascular tissues remaining, whilst sclerotia were formed in the receptacle. This experiment was designed to ensure controlled production conditions that allow evaluation of the metabolic status of the tissues constituting the main entry point of the pathogen (sunflower florets) at early stages of the infection process, prior to the detection of visual symptoms in the *capitulum*.

2.2. Small molecule metabolite detection in sunflower capitula by gas chromatography–mass spectrometry

Following confirmation that the selected genetic material exhibited contrasting behavior with respect to the pathogen, we adapted and optimized a GC–MS method previously established for different tissues of several dicotyledonous species (including *Arabidopsis*, tomato and potato; Lisec et al., 2006; Lytovchenko et al., 2002; Roessner et al., 2001; Roessner-Tunali et al., 2003; Schauer et al., 2006). In order to validate that the previously established method was also suitable for the analysis of sunflower tissue, a recombination experiment was also carried out in which extracts from tomato fruits and sunflower florets were subjected

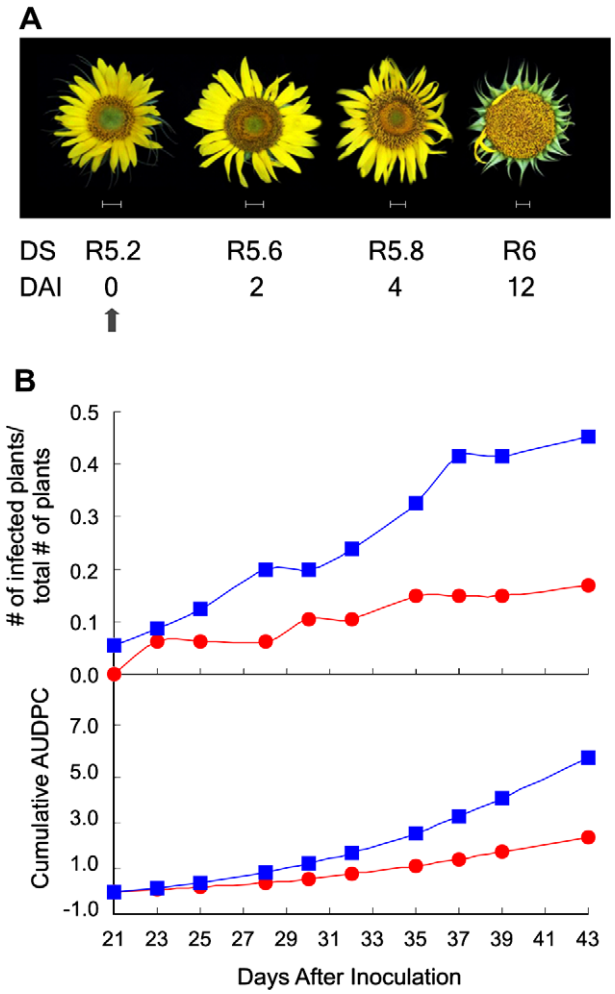

Fig. 1. (A) Experimental design. Sunflower plants were grown under field conditions and capitula were inoculated at developmental stage (DS) R5.2 with an ascospore suspension of 2500 ascospore/ml (indicated by a grey arrow). Floret material was sampled at 0, 2, 4 and 12 days after inoculation (DAI). Size bars represent 1 cm. B. Disease progress curve (above) and calculated cumulative AUDPC (Area under the Disease Progress Curve) (below). Red and blue symbols represents values calculated for RHA801 and HA89 genotypes, respectively. (For interpretation of the references to colour in this figure legend, the reader is referred to the web version of this article.)

to GC–MS analysis both in isolation (Supplementary Fig. 1A and B) and subsequently as a stoichiometrically equivalent mixture (Supplementary Fig. 1C). This experiment served two purposes (i) it allowed assessment that peak identification for sunflower samples was equivalent to that for tomato fruit and (ii) it allowed an analysis of the effectiveness of the extraction protocol for the novel tissue. Sunflower peaks nicely aligned to those we had previously annotated in the tomato fruit (Supplementary Fig. 1C). Moreover, the second analysis demonstrated that the relative values determined in the simple sunflower extracts could be quantifiably retrieved in the mixed extract, with the vast majority of the 63 chemicals being recovered at between 70% and 130% of the level at which they were added. This validation gave similar results to those previously obtained on comparison of tomato and potato tissue (Roessner-Tunali et al., 2003). In addition to the metabolites common to both tissues, a number of peaks that were below the limit of the detection level in the tomato fruit extracts used here (namely homo-serine, 2-oxoglutarate, fucose/rhamnose, t-caffeate, gentiobiose, maltitol, isomaltose, chlorogenate and raffinose), were identified in sunflower florets by comparison with a range of available mass spectral libraries (see Tohge and Fernie, 2009 for listings).

In summary, 63 metabolites could be identified by the use of retention index (RI) method and mass similarity (Fiehn et al., 2000; Wagner et al., 2003) from which we reliably quantified the levels of 50 metabolites (out of those 63 identified) of known chemical structure including 16 amino acids, 16 organic acids, eight di- and trisaccharides, four sugar alcohols, four phosphorylated intermediates and two fatty acids.

2.3. Metabolite variations in sunflower tissues infected with *S. sclerotiorum*

Florets are the first target tissues colonized by *S. sclerotiorum* well before the sunflower head rot disease can be detected in the *capitulum*. Differential staining and fluorescence microscopy techniques (Rodríguez et al., 2004; Pedraza, 2005) demonstrated differences in fungal germination and fungal development in floret sections between susceptible and resistant sunflower genotypes; these were especially prominent following 6 days of inoculation (Rodríguez et al., 2004). The steady-state levels of all identified metabolites at the time of inoculation (0 DAI), two early time points following inoculation (2 and 4 DAI) and a somewhat later time point but one still prior to visualization of disease symptoms (12 DAI) were quantified in the two genotypes. A two-way ANOVA analysis was applied to each metabolite dataset in order to discriminate those effects which were due to genotype from those related either to the progression of infection or to general developmental changes (Table I, Supplementary Material). Multiple comparison tests were also performed whenever a significant result was obtained (Tables II–IV, Supplementary Material).

Differences in steady-state of sugar contents were significantly affected by period of time post-inoculation, with only the levels of trehalose displaying significant differences both between genotypes and time points (Fig. 2). Interaction between the two variables was only detected for sucrose contents, despite the fact that no significant differences in its levels were observed for the HA89 genotype; a decrease was apparent as early as 2 DAI for the RHA801 genotype, followed by a recovery to initial levels by 12 DAI.

Amongst the sugar alcohols quantified here, ononitol displayed a significant *F*-value for the genotype effect with the resistant genotype showing higher contents, particularly at 2 and 4 DAI (Fig. 2).

Phosphorylated intermediates were hardly altered between the lines, although a trend towards higher levels of these metabolites in the initial days after inoculation was observed for the susceptible genotype. Levels of myo-inositol-1-phosphate were affected by both genotype and also by time period following inoculation. Contents of this metabolite were significantly higher in the HA89 genotype at 2 DAI. Fructose-6-phosphate displayed a significant interaction effect (Fig. 2).

Levels of the TCA cycle organic acids showed a coordinated pattern of change in the two genotypes examined, with several of these metabolites peaking at 2 or 4 DAI but decreasing dramatically thereafter. Of particular note are succinate, citrate and isocitrate, which are present at markedly higher levels in RHA801 (Fig. 2). A significant interaction between effects was observed for the content of isocitrate; in the resistant genotype, a significant increment in this compound was detected at 4 DAI followed by a subsequent decrease at 12 DAI, whereas for HA89 the only change detected was the decrease at 12 DAI. Furthermore, comparisons between the genotypes at equivalent time-points indicated that RHA801 contained significantly higher contents of isocitrate at both 4 and 12 DAI.

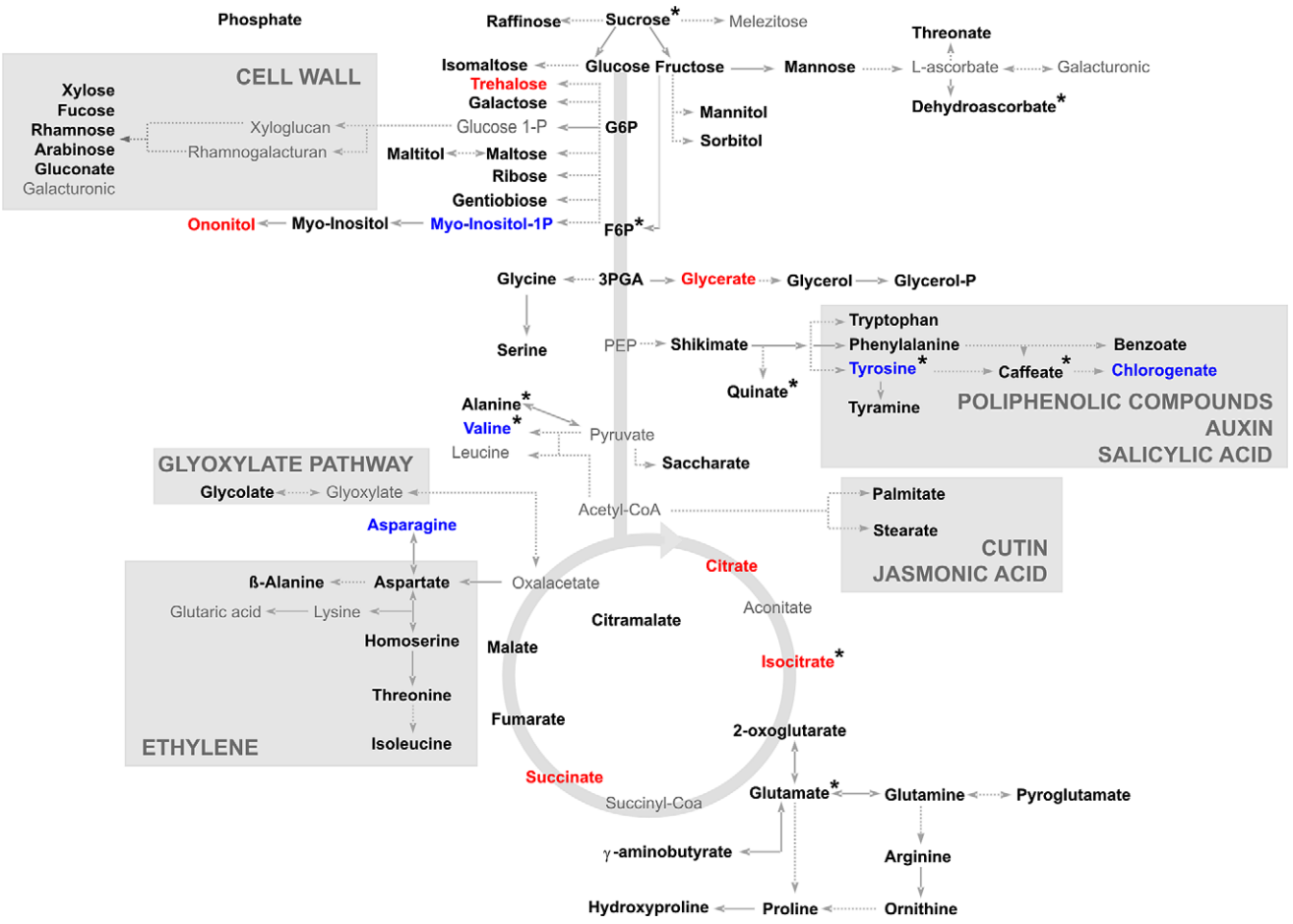

Fig. 2. Schematic representation of the network of metabolic pathways analyzed in sunflower florets. Sugars, sugar-phosphates, sugar-alcohols, amino, organic and fatty acids and few secondary metabolites were identified as shown in Supplementary Fig. 2 and are indicated in bold fonts. Names in gray font indicate that the corresponding metabolite was not determined but are included in the graph for explanatory reasons only. Names in red and blue fonts indicate those metabolites significantly increased in the RHA801 and HA89 genotypes, respectively. Asterisk denotes metabolites for which interaction between genotype and DAI were found. (For interpretation of the references to colour in this figure legend, the reader is referred to the web version of this article.)

Changes in the levels of non-TCA cycle organic acids displayed mixed behavior; however, the major discriminating factor appears to be days after inoculation. Significant differences were observed between time points in the metabolites gluconate, saccharate and threonate, whereas both days after inoculation and genotype affected glycerate and chlorogenate contents; dehydroascorbate, quinate and t-caffeate exhibited significant interactions between the variables under study.

With respect to amino acids, valine, tyrosine and asparagine showed higher levels in the susceptible line whilst the first two plus alanine and glutamate showed significant interactions between genotype and days following inoculation.

In sum, the group of metabolites showing significant effects associated with the genotype (highlighted in red and blue types in Fig. 2) could potentially discriminate sunflower inbred lines RHA801 and HA89 on the basis of infection-dependent changes in metabolism and thus can be postulated as metabolic markers.

2.4. Principal component analysis (PCA) and hierarchical cluster analysis (HCA) of the metabolic complement of infected flowers tissues in resistant and susceptible sunflower genotypes

Given that one of the primary objectives of this study was to evaluate the metabolic complements of sunflower genotypes with contrasting degree of resistance to *S. sclerotiorum* infection, we next applied multivariate non-parametric statistical tools to our combined data set. Principal component analysis (PCA) (Fig. 3A) showed that biological samples (harvested from independent plants) from the same genotype and time point grouped together for the HA89 genotype and this could be clearly distinguished in two-dimensions explaining more than 70% of the variability in the data set. Although at the first time point (0 DAI), samples harvested from the resistant genotype (RHA801) grouped together, at later points samples from this genotype could not be clearly discriminated.

In a complementary approach, hierarchical cluster analysis (HCA) was performed (Fig. 3B). Application of cluster analysis to the mean metabolite data of each treatment gave several interesting observations. According to HCA, at the first time point (0 DAI), the metabolite complement of the resistant genotype exhibited greater similarity to the cluster composed by the susceptible genotype at 0, 2 and 4 DAI than to its own counterparts. However, within a short period after inoculation, RHA801 representatives clustered together. Interestingly, samples harvested from both genotypes after 12 DAI showed no association with either of the two clusters (Fig. 3B).

2.5. Correlative behavior in metabolite levels suggests differential regulation of distinct metabolic pathways between genotypes

Results described above allow quantitative interpretation of metabolite levels of two sunflower genotypes with contrasting

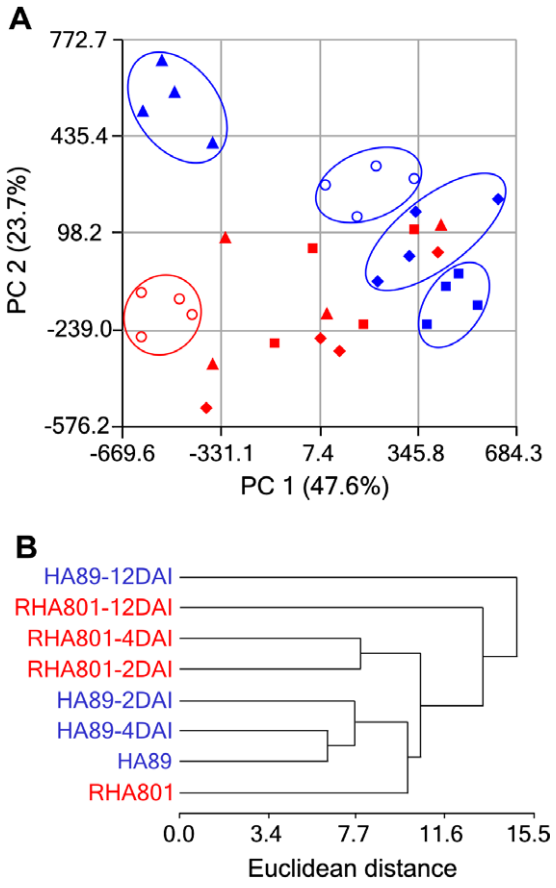

Fig. 3. (A) PCA of the metabolite profiles of all analysed sunflower florets. Red and blue symbols denote samples from RHA801 and HA89 genotypes, respectively. Empty circles correspond to samples taken from non-infected control plants. Triangles, squares and diamonds correspond to samples harvested 2, 4 and 12 DAI, respectively. PC: principal component. PCA vectors span a three-dimensional space to afford best sample separation. Vectors 1 and 2 including 71.3% of the metabolic variance are presented here. (B) Dendrogram obtained after HCA of the metabolic profiles of the analysed sunflower system. The distances between these populations were calculated as described in the Section 5 using the normalized data of averaged measurements. (For interpretation of the references to colour in this figure legend, the reader is referred to the web version of this article.)

behavior to sunflower head rot disease. The data, however, also facilitate an in-depth evaluation of the behavior of the metabolic network by means of assessing the pair-wise correlation of each metabolite within the data set. Of the 989 and 928 possible non-redundant pairs analyzed for each genotype, 109 and 175 displayed *p*-values below 0.01 in HA89 and RHA801 genotypes, respectively; this is considerably higher than the number that would be expected merely by chance. Of these metabolites, only 23 and 14 showed negative correlation coefficients in HA89 and RHA801, respectively. However, following application of the highly stringent Bonferroni correction (Rice, 1989), a total of 13 and 35 significant associations (overall $\alpha = 0.1$) were detected for HA89 and RHA801, respectively, (Table V Supplementary Material).

Results obtained from these analyses are presented in the heatmaps of Fig. 4 and in Supplementary Table V. Whilst it should be borne in mind that the dataset used here is somewhat small in size for such a purpose, a detailed evaluation of these correlations gave several interesting trends. Out of the total significant correlations, only 38 (less than 40%) were shared by both the resistant and susceptible lines, whilst most of them were genotype-specific. Indeed, when correlation coefficients are grouped by the number and nature of connections by using the cartographical representation method proposed by Guimerà and Nunes Amaral (2005), different pictures for each genotype can be seen. Three and four modules, where a module is defined as a subset of metabolites that are connected more to each other than to metabolites in other modules, were distinguished for the resistant and the susceptible lines, respectively. Whilst module 4 of HA89 line and 3 of RHA801 line are essentially the same (except for the presence of a connection to glycolate in the HA89 line), other modules were both qualitatively and quantitatively quite distinct between genotypes. The density of lines crossing the circular network connecting modules in the susceptible cultivar (Fig. 4A) shows that the number of connections between metabolites is almost the same both within and outside a given module. However, connections between different modules are essentially represented by negative correlations (12 out of 15 significant correlations). Although the resistant cultivar displayed a total higher number of significant correlations in comparison with the susceptible one, connections between modules are clearly fewer than those within modules and furthermore, all of the correlations are positive (Fig. 4B).

The TCA cycle intermediates 2-oxoglutarate, succinate, malate and the amino acid glutamate are centers of multiple correlations in both genotypes (Fig. 4 and Supplementary Table V), whereas other metabolites can be considered genotype-specific correlation centers ("hubs"). In the case of the susceptible cultivar, for example, the amino acids isoleucine and homo-serine, the organic acids quinate and citrate and the monosaccharide rhamnose were highly connected. In contrast, in the resistant cultivar there were rather the amino acids glycine and hydroxyproline, the polyols maltitol, glycerol and ononitol, the monosaccharide arabinose and the monoamine compound tyramine that displayed hub-like behavior (Fig. 4). When taken together, these analyses clearly show a differential synchronization in the metabolic patterns of the floret cells in the evaluated genotypes.

2.6. Measurement of enzyme activities

Both parametric and non-parametric analyses described above suggest that sunflower floret cells reprogram its primary metabolism when challenged with the pathogen. To better understand some of the changes detected in the different metabolic pathways, we determined activities of key enzymes of the primary carbon (sucrose synthase and cell wall, cytosolic and vacuolar invertases), photorespiratory (catalase) and phenylpropanoid (phenylalanine ammonia-lyase -PAL-) metabolism at early time points after inoculation (from 0 to 4 DAI) (Table 1). There were significant increases detected in the maximal catalytic activities of vacuolar and cytosolic invertases of about 34% and 40%, respectively, when comparing mock and inoculated samples at 4 DAI in the susceptible genotype HA89. However, no differences were detected in the resistant cultivar. There were no changes observed in the activities of the two other enzymes of sucrose catabolism – cell wall invertase and sucrose synthase. Regarding the activity of H_2O_2 scavenging enzymes, a significant threefold increase in the catalase activity of the resistant genotype RHA801 was also observed at 4 DAI. By contrast, PAL activity was significantly reduced by about 50% at 1 DAI in the resistant genotype. No significant differences were observed in the activities of these two enzymes in the susceptible line challenged with the pathogen.

3. Discussion

This study illustrates the potential of broad based metabolite profiling in the analysis of metabolic changes associated to *S. sclerotiorum* infection in sunflower. Using an established GC–MS-based metabolic profiling approach, we evaluated the primary metabolism of florets of two sunflower inbred lines grown under

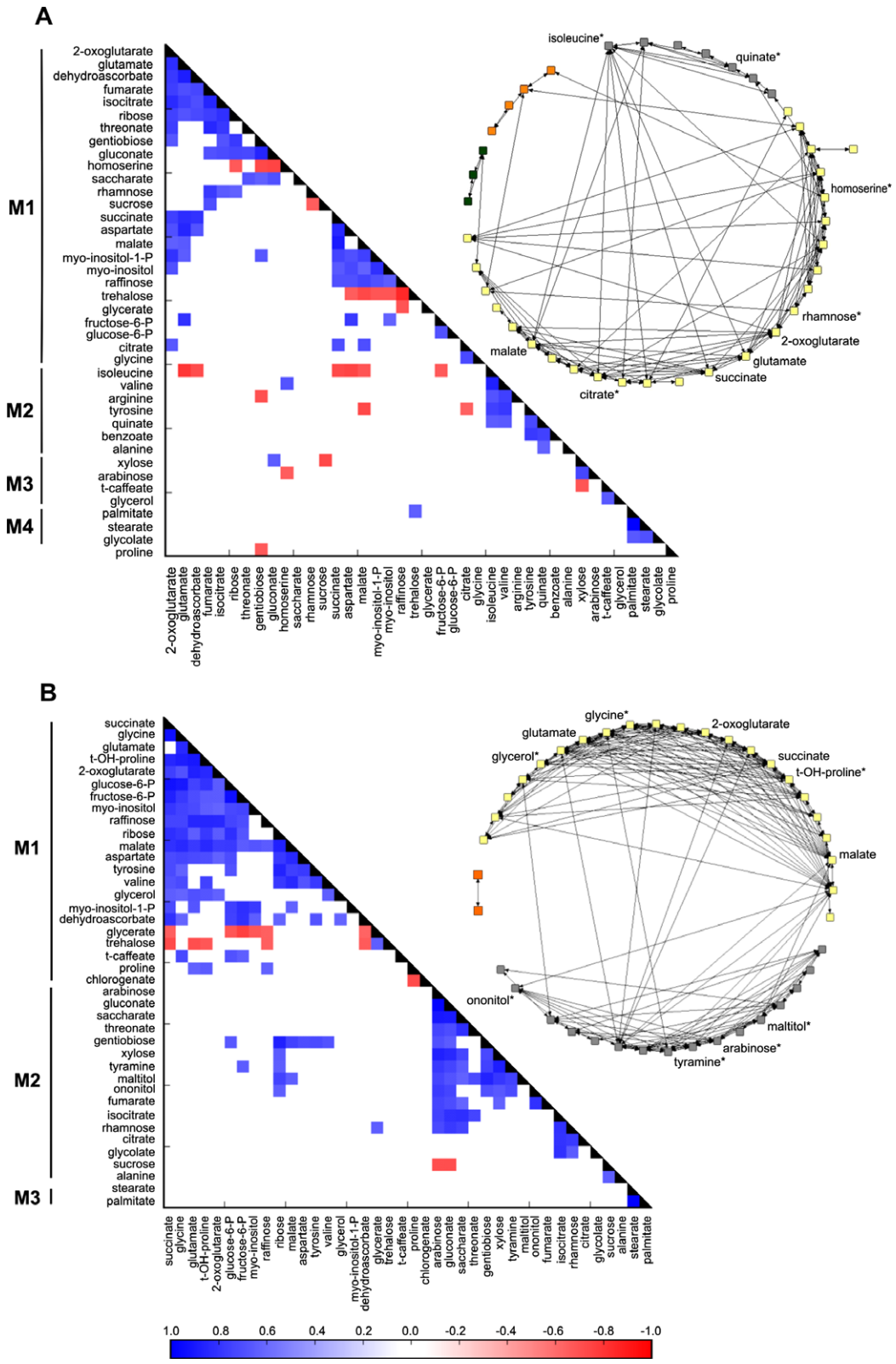

Fig. 4. Visualization of significant metabolite–metabolite correlations ($p < 0.01$) (left) and circular network representations (right) of two sunflower genotypes with contrasting behavior to head rot disease caused by *S. sclerotiorum*. (A) HA89 (susceptible). (B) RHA801 (resistant). Each dot-square of the heatmaps represents the correlation coefficients between metabolites in a false colour scale. Metabolites were ordered according to the modules (M) identified as explained in the Section 5. Different colours depict modules of the circular networks: module 1 (M1) yellow, module 2 (M2) grey, module 3 (M3) orange and module 4 (M4) green. Lines between metabolites represent significant correlations between metabolites. Labels are given for those metabolites identified as hubs and are marked with an asterisk. (For interpretation of the references to colour in this figure legend, the reader is referred to the web version of this article.)

field conditions upon *S. sclerotiorum* inoculation. Jobic et al. (2007) have previously reported the application of a NMR spectrometry approach for profiling the sunflower–*S. sclerotiorum* interaction system, in which they were able to detect 28 different small

Table 1
Enzyme activities in florets of sunflower genotypes. Enzyme activities were determined in florets sampled at indicated times after inoculation. Presented data are means ± SE of measurements from three to six independent samples per genotype. Bold types indicate those that were determined by the Student's *t* test ($p < 0.05$) to be significantly different between mock and inoculated samples. Nd: not detected. –: not measured.

	Mock				Inoculated		
	Days after inoculation						
	0	1	2	4	1	2	4
Sucrose synthase (nmol UDP-glu min^{-1} mg $protein^{-1}$)							
HA89	8.59 ± 0.78	–	–	9.34 ± 0.56	–	–	9.42 ± 0.96
RHA801	7.30 ± 0.66	–	–	10.82 ± 0.51	–	–	9.48 ± 1.17
Cell wall invertase (μmol reducing sugars min^{-1} g DW^{-1})							
HA89	2.87 ± 010	–	–	2.69 ± 0.02	–	–	2.78 ± 0.06
RHA801	2.75 ± 0.03	–	–	2.35 ± 0.10	–	–	2.41 ± 0.15
Cytosolic invertase (nmol reducing sugars min^{-1} mg $protein^{-1}$)							
HA89	0.51 ± 0.01	–	–	**0.20 ± 0.01**	–	–	**0.28 ± 0.02**
RHA801	0.59 ± 0.05	–	–	0.43 ± 0.13	–	–	0.40 ± 0.03
Vacuolar invertase (nmol reducing sugars min^{-1} mg $protein^{-1}$)							
HA89	1.13 ± 0.05	–	–	**0.50 ± 0.02**	–	–	**0.67 ± 0.04**
RHA801	1.46 ± 0.09	–	–	0.98 ± 0.22	–	–	1.04 ± 0.07
Catalase (Units mg $protein^{-1}$)							
HA89	3.93 ± 0.39	5.36 ± 0.83	4.72 ± 0.62	4.37 ± 1.14	3.18 ± 0.71	5.46 ± 1.03	4.25 ± 0.55
RHA801	2.64 ± 0.64	2.51 ± 0.32	2.57 ± 0.27	**1.88 ± 0.22**	3.61 ± 0.61	2.38 ± 0.32	**5.65 ± 1.21**
Phenylalanine ammonia-lyase (nmol cinnamic acid min^{-1} μg $protein^{-1}$)							
HA89	1.66 ± 0.04	0.58 ± 0.09	1.20 ± 0.18	0.69 ± 0.09	0.24 ± 0.07	0.91 ± 0.05	0.27 ± 0.02
RHA801	0.63 ± 0.01	**0.65 ± 0.05**	nd	nd	**0.34 ± 0.08**	0.11 ± 0.02	nd

molecules. Despite distinct advantages and disadvantages of NMR and GC–MS approaches, these strategies have been proposed as complementary technologies for metabolic profiling, especially in the context of biomarker discovery (Fernie et al., 2004; Meyer et al., 2007). Although about 15 common metabolites were quantified in the present work and in the previously mentioned study, the vast majority of metabolites were exclusively detected by our GC–MS approach.

A compendium of recent reports has provided considerable evidence about the key role of primary metabolic pathways in plant defense (Depuydt et al., 2009; Kocal et al., 2008; Scheideler et al., 2002; Price et al., 2003; Lipka et al., 2005; Chandra-Shekara et al., 2007; Kachroo et al., 2004; Kachroo et al., 2008), enhancing the importance of the different profiling approaches for more comprehensive metabolic studies in host–pathogen systems.

Whilst many metabolic profiling studies of host–pathogen relationships have been performed focusing on interactions with biotrophs (Bednarek et al., 2005; Jubault et al., 2008; Pedras et al., 2008) and symbiotic microorganisms (Desbrosses et al., 2005), those involving necrotrophic pathogens are limited to date. Furthermore, whilst Jobic et al. (2007) studied metabolic changes of sunflower cotyledons, little is known regarding the metabolic response in sink organs in general. This later point is of particular relevance given that developing flowers are the main entry point of the pathogen causing sunflower head rot disease. In the present study, compounds involved in primary carbon metabolism of susceptible and resistant sunflower genotypes were analyzed. Moreover, a small number of metabolites showing statistical significant genotype effects could be extracted from the entire profile, and have the potential to discriminate sunflower inbred lines RHA801 and HA89 on the basis of infection-dependent changes in metabolism. As demonstrated in other systems (for a review see Lindon et al., 2004) they furthermore, could be developed into rapidly accessible biomarkers with high predictive power for a complex trait.

A global analysis of the whole dataset using PCA and HCA indicated both metabolic differences between resistant and susceptible genotypes immediately before inoculation (0 DAI) and concerted, yet differential patterns of changes between host–pathogen interactions at very early stages after inoculation. Moreover, network correlation analyses suggest that metabolic changes are synchronized in a time course dependent manner in response to the pathogen, particularly in the susceptible line HA89. This could either be a consequence of pre-existing metabolic differences between the genotypes or due to induced changes by the infection process.

Correlation network analysis also allowed the identification of differential patterns for several metabolites (i.e. 2-oxoglutarate, succinate, malate and glutamate) constituting hubs common to the two evaluated genotypes. Interestingly, all these metabolites belong to the same routes – TCA cycle linked to glutamate metabolism – suggesting that these steps of the pathway are not directly linked to the observed differences in pathogen resistance and have conserved roles in both lines. However, TCA cycle intermediates maintained expected stoichiometry in the susceptible genotype, in the resistant one they were more variable with respect to one another hinting at metabolic regulation within the pathway. This could suggest a differential respiratory rate between the genotypes and an infection–elicited oxidative burst. This hypothesis is supported by the fact that the H_2O_2 scavenging enzyme catalase displayed a markedly increased activity in florets of the resistant genotype when challenged with the pathogen, suggesting that metabolism is reconfigured to bypass the oxidative burst within the cells of this cultivar. An extensive inhibition of the TCA cycle has previously been demonstrated in *Arabidopsis* cell suspensions subjected to oxidative stress (Baxter et al., 2007), and differential regulation of the enzyme encoding genes involved in this pathway has also been well documented in different plant–pathogen interaction systems (see for example Rhoads et al., 2006; Scheideler et al., 2002).

Interestingly, most of the metabolites identified as genotype-specific hubs have been shown to be implicated in signaling pathways regulating various aspects of plant defense. Citrate, isoleucine, quinate, homo-serine and rhamnose exhibited the highest number of genotype-specific connections in the correlation network analysis of the susceptible line. A shift in the carbon/nitrogen balance has been proposed as a general plant response to pathogen infections via a differential regulation of the enzyme encoding genes of many different primary pathways as the TCA cycle and amino acids metabolism (Zhu et al., 2007). Moreover, isoleucine conjugated –jasmonate and –glucosinolates have recently been implicated in plant response to insect herbivores and pathogens (Chung et al., 2008; Mikkelsen and Halkier, 2003).

Phenylpropanoids belong to the largest group of secondary metabolites produced by plants, mainly in response to biotic stresses by their antioxidant and free radical scavenging properties (for a review see Korkina, 2007). Precursors of phenylpropanoid pathways gave a differential response in the current study. Tyrosine levels increased threefold at later stages in the susceptible line whilst other precursor metabolites such as chlorogenate also showed a differential pattern of changes in this line. Sunflower resistant genotypes have shown higher constitutive and induced soluble phenolic content in bracts (Prats et al., 2003, 2007), as well as increased phenylalanine ammonia-lyase activity but not prior to 10–14 DAI (Prats et al., 2003). However, our results of enzyme activity measurement suggest that PAL seems not to be directly involved in this mechanism in florets, at least not in the first stages following infection. The observed changes in levels of phenylpropanoid precursors in our experiments might lead to a differential biosynthesis of other defense and developmental related hormones such as salicylate and auxins.

Analyzing the correlation network of the resistant line, it was revealed that glycerol, ononitol, maltitol, glycine, hydroxiproline, arabinose and tyramine were highly connected. Glycerol and ononitol are polyalcohols that have been suggested to mediate responses to biotic (Kachroo et al., 2004; Kachroo et al., 2008) and abiotic (Sheveleva et al., 1997) stresses. Exogenous application of glycerol triggered constitutive expression of pathogenesis-related genes in soybean plants, and these plants also showed resistance to bacterial and oomycete pathogens (Kachroo et al., 2008).

It is well accepted that photorespiration forms part of the dissipatory mechanisms of plants to minimize production of reactive oxygen species (ROS) in the chloroplast and to mitigate oxidative damage. Considering that ROS production is triggered by *Sclerotinia*-derived oxalate (Kim et al., 2008), the fact that the photorespiratory intermediate glycine is acting as a specific hub in the resistant genotype hints that it may play a role in mediating defense mechanism/s against this pathogen. This is additionally supported by the increased catalase activity observed in this line upon infection. Thus, photorespiratory regulation could explain, at least in part, the resistant behavior of this genotype to *Sclerotinia.* In addition to oxalate, cell-wall-degrading enzymes are known to be involved in pathogenesis and fungal development (Godoy et al., 1990). Consequently an increment in the levels of cell-wall-derivatives occurs upon infection. In agreement, arabinose levels vary in a coordinate fashion with a high number of metabolites in the RHA801 line. Moreover, the correlations observed for most of the measured cell-wall components (xylose, rhamnose and gluconate) fall into the same module (M2) in the network analysis of this genotype.

Differences in the steady-state levels of single metabolites between the two evaluated genotypes also highlight the importance of analyzing the carbon and nitrogen metabolism and its connection with secondary metabolism.

The resistant genotype showed changes in sucrose content after inoculation similar to those previously observed following pathogenic challenge and demonstrated to be due to the activity of sink-specific cell wall invertases as a general response (Fotopoulos et al., 2003; Roitsch et al., 2003; Scholes et al., 1994; Voegele et al., 2006). Neither invertases nor Susy measured here showed changes in this genotype when compared mock against inoculated samples. By contrast, the susceptible genotype showed significant decreased levels in the activity of cytosolic and vacuolar invertases. However, these results do not correlate with the steady-state levels of sucrose detected in this genotype. Although this is somewhat unexpected, it has been reported that the effect of pathogen infection on sugar levels varies considerably between different plant–pathogen interactions (for a review see Berger et al., 2007). Moreover, the analysis of sugar levels and invertase activity in infected *versus* uninfected regions of inoculated tissues showed only strong effects in the infected region (Chou et al., 2000; Swarbrick et al., 2006). This accounts for the need of methods providing information on the spatial distribution of compounds on the organ-, tissue-, and sub-cellular level to elucidate these effects.

Nitrogen recycling and mobilization in host plants during pathogen attack and invasion are well documented as a defense strategy (Divon et al., 2006 and references therein). Intriguingly, the levels of metabolites of the cell nitrogen status (such as glutamate and asparagine) showed contrasting, yet unexpected, behaviors in the genotypes analyzed here. While in the susceptible genotype these two amino acids increased upon inoculation, the opposite occurred in the resistant line providing further evidence in support of the idea that N-remobilization is differentially triggered in compatible and incompatible interactions (Tavernier et al., 2007). In a compatible *Arabidopsis thaliana–Plasmodiophora brassicae* interaction it was also suggested that enhancement of the metabolic flux from arginine to proline is associated with induced susceptibility through induced degradation of arginine to ammonium and ornithine, thus providing a mechanism to divert plant nitrogen into the production of amino acids indispensable for pathogen multiplication (Jubault et al., 2008). In the present study, the steady state increment through the infection process of proline in the susceptible genotype compared to the resistant one is in agreement with those results reported in other compatible systems and could play an important role as determinant of susceptibility of sunflower to *S. sclerotiorum* infections.

In order to better define specific responses in this pathosystem, a population derived from a cross between these contrasting genotypes is being carried out. It is expected that the metabolite profile method established here will permit the analysis of these segregants and help to fully confirm the specificity of the metabolic changes described here.

4. Conclusions

The lack of knowledge concerning the metabolism of the main *S. sclerotiorum* entry point in sunflower led us to apply a GC–MS method for metabolite profiling. This method allowed us to characterize the metabolic profiles in inoculated *capitula* of two genotypes with contrasting resistance levels to *S. sclerotiorum* infection. Upon applying parametric statistics analysis this study allowed to distinguish metabolic patterns that could potentially discriminate sunflower genotypes on the basis of infection-dependent changes of metabolism.

Non-parametric analysis allowed us to detect differential metabolic regulation between susceptible and resistant genotypes in the sunflower-*Sclerotinia* system. Primary metabolic events in floret cells are differentially synchronized in genotypes with contrasting behaviors tested under field conditions. Network analyses further extended our initial hypothesis of the notion of a metabolic signature triggered by the pathogen in sunflower plants under field conditions, and thus may ultimately have important implications for crop breeding.

5. Experimental

5.1. Plant material

The two inbred lines used in this study were originally provided by J. Miller (NDSU, ND, USA). HA89 has been released as a maintainer line described as susceptible to different diseases (Oils Seed Sunflower, ND Experimental Station, NDSU, USA). RHA801 is a restoration line selected from a restored population obtained from

the following four parental lines: RHA271, RHA273, RHA274, R344 and R494.

5.2. Pathogenic material

A population of *S. sclerotiorum* from Balcarce (Buenos Aires, Argentina) was used. The sclerotia were collected in the field and stored in paper bags at 13 °C for 3 months. For apothecium production, the procedure used by Escande et al. (2002) was followed. Shortly, sclerotia were exposed at −18 ± 2 °C for 7 days and buried 1 cm deep in humid pasteurized soil until stile emergence. Cultures were incubated at 16 °C and approximately 2500 lux of continuous daylight. Mature apothecia were harvested and positioned upside down in glass Petri dishes for 4 h to favour ascospores releasing. Ascospores were stored in Petri dishes at −18 °C until use. For inoculation of flowers, ascospores were suspended in sterile distilled water to a concentration of 2500 spores/ml.

5.3. Field experiment

The field experiment was conducted at INTA – Balcarce Experimental Station (Province of Buenos Aires, Argentina) following seed and plant care as described by Maringolo (2007). Sunflower seeds from both lines were sown in the experimental field in completely randomized plots, in typical Argiudol soil containing 5% organic matter at pH 6.2, in rows 8 m long with plants spaced at 20 cm apart within the row and 75 cm apart between rows. Sunflower heads were randomly chosen from the rows and sprayed with inoculum at R5.2 stage according to Schneiter and Miller scale (Schneiter and Miller, 1981), with two outer rows of florets in anthesis and the crop was maintained under high humidity conditions by sprinkler irrigation. *Capitula* were harvested immediately (0) and 2, 4 and 12 days after inoculation (DAI). Four pools of 10 *capitula* were sampled. They were immediately frozen in liquid N_2 and kept at −80 °C until processed. During the sampling period neither lesions nor mycelia were observed on the *capitulum* surfaces.

On basis of the severity measurements, the AUDPC was calculated according to the equation of Campbell and Madden (1990):

$$\mathrm{AUDPC} = \sum_{i}^{n-1} (y_i + y_{i+1})/2 \times (t_{i+1} - t_i)$$

where n is the number of evaluations, y the severity or incidence and t the number of days after sowing where at each evaluation. $(t, y) = (0, 0)$ is included as the first evaluation.

5.4. Chemical materials

Except where otherwise stated all enzymes and materials were purchased from Roche (Mannheim, Germany) or Sigma Chemical Company (St. Louis, USA).

5.5. Metabolite analysis

The relative levels of metabolites were determined from frozen sunflower floret samples by GC–MS essentially as described in Lisec et al. (2006), with the following modifications; an extra step of $CHCl_3$ extraction was performed due to the high proportion of non-polar compounds found in sunflower florets and two different amounts of extract (2.5% and 5% v/v) were derivatised and injected into the GC–MS to circumvent the occurrence of overloaded peaks which result in low quality data for the more abundant cellular metabolites. Samples (1 μl) were injected in the GC–MS system which consists of an AS2000 autosampler, a GC8000 gas chromatograph and a Voyager quadropole mass spectrometer (ThermoQuest, Manchester, UK). Chromatography was performed on a 30 m SPB-50 column with 0.25 mm inner diameter and 0.25 μm film thickness (Supelco, Belfonte, CA, USA). Injection temperature was 230 °C, the interface set to 250 °C and the ion source adjusted to 200 °C. The carrier gas was He at a constant flow ratio of 1 ml m^{-1}.

The chromatograms and spectra were evaluated using the MASSLAB software (ThermoQuest, Manchester, UK). Data are presented normalized to those of the susceptible genotype under control conditions as described by Roessner et al. (2000). Recombination experiments were performed as detailed in Roessner-Tunali et al. (2003).

5.6. Analysis of enzyme activities

All enzymes were determined in different aliquots of the same harvested samples at 0, 1, 2 and 4 DAI in both genotypes. Vacuolar and cytosolic invertases and sucrose synthase (in the direction of sucrose degradation) were measured as described in Zrenner et al. (1995). Cell wall invertase activity was determined according to Kocal et al. (2008). Catalase activity was measured as described by Aebi (1984). Phenylalanine-ammonia-lyase (PAL) was determined as described in Zucker (1968). Three to six biological replicates were measured.

5.7. Data analyses

Differences in metabolite contents between genotypes and days after inoculation were assessed using a two-factor analysis of variance (Anova) with fixed effects. Two levels were considered for the genotype factor (RHA801: resistant; HA89: susceptible) and four for the DAI factor (0, 2, 4, 12). For those metabolites exhibiting significant main effects ($p < 0.05$) and no interaction between variables, pair-wise comparisons among treatments were conducted using Tukey honest significant difference test. If significant interactions were detected, each factor was analyzed separately within the levels of the other with a one-way Anova and pair-wise comparisons were performed as needed using Tukey test.

HCA (Hierarchical Cluster Analysis) and PCA (Principal Component Analysis) were performed with the software Infostat (v2008 http://www.infostat.com.ar). For the HCA analysis, Euclidean distances were computed using the average from each genotype-time point after inoculation and transformed into log10 to allow better comparison of large and small numbers. The corresponding dendrograms were obtained according to the Unweighted Pair Group Method using arithmetic averages (UPGMA). For PCA, a correlation matrix among variables was computed based on the standardized data matrix and results were then presented as a two-dimensional graphical display of the data in which every symbol represents a defined biological sample.

Pair-wise correlation analysis of metabolites within genotypes was performed using Spearman's coefficient of rank correlation (*rs*) computed with the STATISTICA software package (StatSoft, Tulsa, OK). Pair-wise correlations were performed only for those metabolites quantified in all analyzed time points. Correlation pairs were ranked by Spearman's coefficients and those showing *rs* values = 0 and/or *p*-values = 1 were discarded for further analyses. The 284 correlations (109 and 175 for HA89 and RHA801 genotypes, respectively) that resulted statistically significant were considered for network analyses for each genotype separately. A vertex corresponds to a metabolite and a link between vertices corresponds to significant correlations between two metabolites. The networks were then subjected to the cartographical analysis proposed by Guimerà and Nunes Amaral (2005). Modules were identified by the correlation-based distance measure and the average

linkage clustering method (EPCLUST Vilo et al., 2003). Networks were drawn by using the NetDraw software package (Analytical Technology http://www.analytictech.com/). Hub compounds were defined as those presented a number of connections (significant correlations) above the average. Average connection per metabolite (ACM) were calculated for each genotype separately considering all significant correlations ($p < 0.01$).

Acknowledgments

This work was partially supported with grants from the Max Planck Society (Germany) to ARF and FC, DFG (Germany) to AL, INTA (Argentina) to RAH, ANPCyT (Argentina) to RAH and CONICET (Argentina) to RAH and FC. LP holds a CONICET PhD fellowship. FC, VL, NP and RAH are members of CONICET. HEH, AE, NP and RAH are independent researchers at INTA. We thank Christian Kristukat for help with the Python IDLE software.

Appendix A. Supplementary data

Supplementary data associated with this article can be found, in the online version, at doi:10.1016/j.phytochem.2009.09.018.

References

Abood, J.K., Lösel, D.M., 2003. Changes in carbohydrate composition of cucumber leaves during the development of powdery mildew infection. Plant Pathol. 52, 256–265.

Aebi, H., 1984. Catalase in vitro. Meth. Enzymol. 105, 121–125.

Al-Chaarani, G.R., Roustaee, A., Gentzbittel, L., Mokrani, L., Barrault, G., Dechamp-Guillaume, G., Sarrafi, A., 2002. A QTL analysis of sunflower partial resistance to downy mildew (*Plasmopara halstedii*) and black stem (*Phoma macdonaldii*) by the use of recombinant inbred lines (RILs). Theor. Appl. Genet. 104, 490–496.

Al-Chaarani, G.R., Gentzbittel, L., Huang, X.Q., Sarrafi, A., 2004. Genotypic variation and identification of QTLs of agronomic traits, using AFLP and SSR markers in RILs of sunflower (*Helianthus annuus* L.). Theor. Appl. Genet. 109, 1353–1360.

Baxter, C.J., Redestig, H., Schauer, N., Repsilber, D., Patil, K.R., Nielsen, J., Selbig, J., Liu, J., Fernie, A.R., Sweetlove, L.J., 2007. The metabolic response of heterotrophic *Arabidopsis* cells to oxidative stress. Plant Physiol. 143, 312–325.

Bednarek, P., Schneider, B., Svatos, A., Oldham, L.J., Hahlbrock, K., 2005. Structural complexity, differential response to infection, and tissue specificity of indolic and phenylpropanoid secondary metabolism in *Arabidopsis* roots. Plant Physiol. 38, 1058–1070.

Berger, S., Sinha, A.K., Roitsch, T., 2007. Plant physiology meets phytopathology: plant primary metabolism and plant–pathogen interactions. J. Ex. Bot. 58, 4019–4026.

Bert, P.F., Jouan, I., De Labrouhe, D.T., Serre, F., Nicolas, P., Vear, F., 2002. Comparative genetic analysis of quantitative traits in sunflower (*Helianthus annuus* L.) 1. QTL involved in resistance to *Sclerotinia sclerotiorum* and *Diaporthe helianthi*. Theor. Appl. Genet. 105, 985–993.

Bert, P.F., Dechamp-Guillaume, G., Serre, F., Jouan, I., Tourvieille de Labrouhe, D., Nicolas, P., Vear, F., 2004. Comparative genetic analysis of quantitative traits in sunflower (*Helianthus annuus* L.) 3. Characterisation of QTL involved in resistance to *Sclerotinia sclerotiorum* and *Phoma macdonaldi*. Theor. Appl. Genet. 109, 865–874.

Boland, G.J., Hall, R., 1994. Index of plant hosts of *Sclerotinia sclerotiorum*. Can. J. Plant Pathol. 16, 93–108.

Campbell, C.L., Madden, L.V., 1990. Introduction to Plant Disease Epidemiology. John Willey and Sons, New York.

Carter, C., Thornburg, R.W., 2000. Tobacco nectarin I – purification and characterization as a germin-like, manganese superoxide dismutase implicated in the defense of floral reproductive tissues. J. Biol. Chem. 275, 36726–36733.

Cessna, S.G., Sears, V.E., Dickman, M.B., Low, P.S., 2000. Oxalic acid, a pathogenicity factor for *Sclerotinia sclerotiorum*, suppresses the oxidative burst of the host plant. Plant Cell 12, 2191–2200.

Chandra-Shekara, A.C., Venugopal, S.C., Barman, S.R., Kachroo, A., Kachroo, P., 2007. Plastidial fatty acid levels regulate resistance gene-dependent defense signaling in *Arabidopsis*. Proc. Natl. Acad. Sci. USA 104, 7277–7282.

Chou, H.-M., Bundock, N., Rolfe, S.A., Scholes, J.D., 2000. Infection of *Arabidopsis thaliana* leaves with *Albugo Candida* (white blister rust) causes a reprogramming of host metabolism. Mol. Plant Pathol. 1, 99–113.

Christensen, A.B., Thordal-Christensen, H., Zimmermann, G., Gjetting, T., Lyngkjaer, M.F., Dudler, R., Schweizer, P., 2004. The germin-like protein GLP4 exhibits superoxide dismutase activity and is an important component of quantitative resistance in wheat and barley. MPMI 17, 109–117.

Chung, H.S., Koo, A.J.K., Gao, X., Jayanty, S., Thines, B., Jones, A.D., Howe, G.A., 2008. Regulation and function of *Arabidopsis* JASMONATE ZIM-domain genes in response to wounding and herbivory. Plant Physiol. 146, 952–964.

Depuydt, S., Trenkamp, S., Fernie, A.R., Elftieh, S., Renou, J.-P., Vuylsteke, M., Holsters, M., Vereecke, D., 2009. An integrated genomics approach to define niche establishment by *Rhodococcus fascians*. Plant Physiol. 149, 1366–1386.

Desbrosses, G., Kopka, J., Udvardi, M.K., 2005. *Lotus japonicus* metabolic profiling development of gas chromatography–mass spectrometry resources for the study of plant–microbe interactions. Plant Physiol. 137, 1302–1318.

Divon, H.H., Ziv, C., Davydov, O., Yarden, O., Fluhr, R., 2006. The global nitrogen regulator, FNR1, regulates fungal nutrition-genes and fitness during *Fusarium oxysporum* pathogenesis. Mol. Plant Pathol. 7, 485–497.

Dumas, B., Sailland, A., Cheviet, J.P., Freyssinet, G., Pallett, K., 1993. Identification of barley oxalate oxidase as a germin-like protein. Comptes Rendus de l'Academie des Sciences Serie III-Sciences de la Vie 316, 793–798.

Dutton, M.V., Evans, C.S., 1996. Oxalate production by fungi: its role in pathogenicity and ecology in the soil environment. Can. J. Microbiol. 42, 881–895.

Escande, A.R., Laich, F.S., Pedraza, M.V., 2002. Field testing of honeybee-dispersed *Trichoderma* spp. to manage sunflower head rot (*Sclerotinia sclerotiorum*). Plant Pathol. 51, 346–351.

Fernie, A.R., 2007. The future of metabolic phytochemistry: larger numbers of metabolites, higher resolution, greater understanding. Phytochemistry 68, 2861–2880.

Fernie, A.R., Trethewey, R.N., Krotzky, A.J., Willmitzer, L., 2004. Metabolite profiling: from diagnostics to systems biology. Nat. Rev. Mol. Cell Biol. 5, 1–7.

Fiehn, O., Kopka, J., Dörmann, P., Altmann, T., Trethewey, R.N., Willmitzer, L., 2000. Metabolite profiling for plant functional genomics. Nat. Biotechnol. 18, 1157–1161.

Fotopoulos, V., Gilbert, M.J., Pittman, J.K., Marvier, A.C., Buchanan, A.J., Sauer, N., Hall, J.L., Williams, L.E., 2003. The monosaccharide transporter gene, AtSTP4, and the cell-wall invertase, Atβfruct1, are induced in arabidopsis during infection with the fungal biotroph *Erysiphe cichoracearum*. Plant Physiol. 132, 821–829.

Gentzbittel, L., Mouzeyar, S., Badaoui, S., Mestries, E., Vear, F., Tourvieille De Labrouhe, D., Nicolas, P., 1998. Cloning of molecular markers for disease resistance in sunflower, *Helianthus annuus* L. Theor. Appl. Genet. 96, 519–525.

Godfrey, D., Able, A.J., Dry, I.B., 2007. Induction of a grapevine germin-like protein (VvGLP3) gene is closely linked to the site of *Erysiphe necator* infection: a possible role in defense? MPMI 20 (9), 1112–1125.

Godoy, G., Steadman, J.R., Dickman, M.B., Dam, R., 1990. Use of mutants to demonstrate the role of oxalic acid in pathogenicity of *Sclerotinia sclerotiorum* on *Phaseolus vulgaris*. Physiol. Mol. Plant Pathol. 37, 179–191.

Guimerà, R., Nunes Amaral, L.A., 2005. Functional cartography of complex metabolic networks. Nature 433, 895–900.

Hall, J.L., Williams, L.E., 2000. Assimilate transport and partitioning in fungal biotrophic interactions. Aust. J. Plant Pathol. 27, 549–559.

Hu, X., Bidney, D.L., Yalpani, N., Duvick, J.P., Crasta, O., Folkerts, O., Lu, G., 2003. Overexpression of a gene encoding hydrogen peroxide-generating oxalate oxidase evokes defense responses in sunflower. Plant Physiol. 133, 170–181.

Jobic, C., Boisson, A.M., Gout, E., Rascle, C., Fevre, M., Cotton, P., Bligny, R., 2007. Metabolic processes and carbon nutrient exchanges between host and pathogen sustain the disease development during sunflower infection by *Sclerotinia sclerotiorum*. Planta 226, 251–265.

Jubault, M., Hamon, C., Gravot, A., Lariagon, C., Delourme, R., Bouchereau, A., Manzanares-Dauleux, M.J., 2008. Differential regulation of root arginine catabolism and polyamine metabolism in clubroot-susceptible and partially resistant *Arabidopsis* genotypes. Plant Physiol. 146, 2008–2019.

Kachroo, A., Daqi, F., Havens, W., Navarre, D., Kachroo, P., Ghabrial, S., 2008. An oleic acid–mediated pathway induces constitutive defense signaling and enhanced resistance to multiple pathogens in soybean. Mol. Plant Microbe Interact. 21, 564–575.

Kachroo, A., Venugopal, S.C., Lapchyk, L., Falcone, D., Hildebrand, D., Kachroo, P., 2004. Oleic acid levels regulated by glycerolipid metabolism modulate defense gene expression in *Arabidopsis*. Proc. Natl. Acad. Sci. USA 101, 5152–5157.

Kiani, S.P., Talia, P., Maury, P., Grieu, P., Heinz, R., Perrault, A., Nishinakamasu, V., Hopp, E., Gentzbittel, L., Paniego, N., Sarrafi, A., 2007. Genetic analysis of plant water status and osmotic adjustment in recombinant inbred lines of sunflower under two water treatments. Plant Sci. 172, 773–787.

Kim, K.S., Min, J.Y., Dickman, M., 2008. Oxalic acid an elicitor of plant programmed cell death during *Sclerotinia sclerotiorum* disease development. Mol. Plant Microbe Interact. 21, 605–612.

Kocal, N., Sonnewald, U., Sonnewald, S., 2008. Cell wall bound invertase limits sucrose export and is involved in symptom development and inhibition of photosynthesis during compatible interaction between tomato and Xanthomonas campestros pv vesicatoria. Plant Physiol. 148, 1523–1536.

Korkina, L.G., 2007. Phenylpropanoids as naturally occurring antioxidants: from plant defense to human health. Cell Mol. Biol. 53, 15–25.

Lindon, J.C., Holmes, E., Bollard, M.E., Stanley, E.G., Nicholson, J.K., 2004. Metabonomics technologies and their applications in physiological monitoring, drug safety assessment and disease diagnosis. Biomarkers 9, 1–31.

Lipka, V., Dittgen, J., Bednarek, P., Bhat, R., Wiermer, M., Stein, M., Landtag, J., Brandt, W., Rosahl, S., Scheel, D., 2005. Pre- and postinvasion defenses both contribute to nonhost resistance in *Arabidopsis*. Science 310, 1180–1183.

Lisec, J., Schauer, N., Kopka, J., Willmitzer, L., Fernie, A.R., 2006. Gas chromatography mass spectrometry-based metabolite profiling in plants. Nat. Protoc. 1, 387–396.

Lytovchenko, A., Bieberich, K., Willmitzer, L., Fernie, A.R., 2002. Carbon assimilation and metabolism in potato leaves deficient in plastidial phosphoglucomutase. Planta 215, 802–811.

Maringolo, C., 2007. QTL Mapping to Resistance to *Sclerotinia* Head Rot of Sunflower (*Sclerotinia sclerotiorum* (Lib.) De Bary). Magister Scientiae Thesis. Facultad de Ciencias Agrarias. Universidad Nacional de Mar del Plata. INTA. Experimental Research Station Balcarce, Argentina.

Mestries, E., Gentzbittel, L., Tourvieille De Labrouhe, D., Nicolas, P., Vear, F., 1998. Analyses of quantitative trait loci associated with resistance to *Sclerotinia sclerotiorum* in sunflowers (*Helianthus annuus* L.) using molecular markers. Mol. Breed. 4, 215–226.

Meyer, R.C., Steinfath, M., Lisec, J., Becher, M., Witucka-Wall, H., Törjék, O., Fiehn, O., Eckardt, A., Willmitzer, L., Selbig, J., Altmann, T., 2007. The metabolic signature related to high plant growth rate in *Arabidopsis thaliana*. Proc. Natl. Acad. Sci. USA 104, 4759–4764.

Micic, Z., Hahn, V., Bauer, E., Melchinger, A.E., Knapp, S.J., Tang, S., Schon, C.C., 2005a. Identification and validation of QTL for *Sclerotinia* midstalk rot resistance in sunflower by selective genotyping. Theor. Appl. Genet. 111, 233–242.

Micic, Z., Hahn, V., Bauer, E., Schon, C.C., Knapp, S.J., Tang, S., Melchinger, A.E., 2004. QTL mapping of midstalk *Sclerotinia* – rot resistance in sunflower. Theor. Appl. Genet. 109, 1474–1484.

Micic, Z., Hahn, V., Bauer, E., Schon, C.C., Melchinger, A.E., 2005b. QTL mapping of resistance to *Sclerotinia* midstalk rot in RIL of sunflower population NDBLOSsel × CM625. Theor. Appl. Genet. 110, 1490–1498.

Mikkelsen, M.D., Halkier, B.A., 2003. Metabolic engineering of valine- and isoleucine-derived glucosinolates in *Arabidopsis* expressing CYP79D2 from cassava. Plant Physiol. 131, 773–779.

Paniego, N., Heinz, R., Hopp, H.E., 2006. Sunflower. In: Kole, C. (Ed.), Genome Mapping and Molecular Breeding Vol. II (Oilseeds). Springer, Berlin, Heidelberg, Germany, pp. 153–178.

Pedras, M.S., Zheng, Q.A., Gadagi, R.S., Rimmer, S.R., 2008. Phytoalexins and polar metabolites from the oilseeds canola and rapeseed: differential metabolic responses to the biotroph *Albugo candida* and to abiotic stress. Phytochemistry 69, 894–910.

Pedraza, M.V., 2005. Estudios tendientes al manejo integrado de la podredumbre húmeda del capítulo del girasol (*Sclerotinia sclerotiorum*). PhD Thesis. Universidad Nacional de Mar del Plata. Facultad de Ciencias Agrarias Balcarce, 102p.

Pereyra, V.R., Escande, A.R., 1994. Enfermedades del Girasol en la Argentina, Manual de Reconocimiento. Instituto Nacional de Tecnologia Agropecuaria Sociedad Impresora Americana, Buenos Aires, Argentina.

Prats, E., Bazzalo, M.E., León, A., Jorrín, J.V., 2003. Accumulation of soluble phenolic compounds in sunflower capitula correlates with resistance to *Sclerotinia sclerotiorum*. Euphytica 132, 321–329.

Prats, E., Bazzalo, M.E., León, A., Jorrin, J.V., 2006. Fungitoxic effect of scopolin and related coumarins on *Sclerotinia sclerotiorum*. A way to overcome sunflower head rot. Euphytica 147, 451–460.

Prats, E., Galindo, J.C., Bazzalo, M.E., Leon, A., Macias, F.A., Rubiales, D., Jorrin, J.V., 2007. Antifungal activity of a new phenolic compound from *capitulum* of a head rot-resistant sunflower genotype. J. Chem. Ecol. 33, 2245–2253.

Price, J., Li, T.C., Kang, S.G., Na, J.K., Jang, J.C., 2003. Mechanisms of glucose signaling during germination of *Arabidopsis*. Plant Physiol. 132, 1424–1438.

Rhoads, D.M., Umbach, A.L., Subbaiah, C.C., Siedow, J.N., 2006. Mitochondrial reactive oxygen species. Contribution to oxidative stress and interorganellar signaling. Plant Physiol. 141, 357–366.

Rice, W., 1989. Analysing tables of statistical tests. Evolution 43, 223–225.

Rodríguez, M.A., Venedikian, N., Bazzalo, M.E., Godeas, A., 2004. Histopathology of *Sclerotinia sclerotiorum* attack on flower parts of *Helianthus annuus* heads in tolerant and susceptible varieties. Mycopathologia 157, 291–302.

Roessner, U., Wagner, C., Kopka, J., Trethewey, R.N., Willmitzer, L., 2000. Simultaneous analysis of metabolites in potato tuber by gas chromatography–mass spectrometry. Plant J. 23, 131–142.

Roessner, U., Luedemann, A., Brust, D., Fiehn, O., Linke, T., Willmitzer, L., Fernie, A.R., 2001. Metabolic profiling allows comprehensive phenotyping of genetically or environmentally modified plant systems. Plant Cell 13, 11–29.

Roessner-Tunali, U., Hegemann, B., Lytovchenko, A., Carrari, F., Bruedigam, C., Granot, D., Fernie, A.R., 2003. Metabolic profiling of transgenic tomato plants overexpressing hexokinase reveals that the influence of hexose phosphorylation diminishes during fruit development. Plant Physiol. 133, 84–99.

Roitsch, T., Balibrea, M.E., Hofmann, M., Proels, R., Sinha, A.K., 2003. Extracellular invertase: key metabolic enzyme and PR protein. J. Exp. Bot. 382, 513–524.

Rönicke, S., Hahn, V., Vogler, A., Friedt, W., 2005. Quantitative trait loci analysis of resistance to *Sclerotinia sclerotiorum* in sunflower. Phytopathology 95, 834–839.

Schauer, N., Semel, Y., Roessner, U., Gur, A., Balbo, I., Carrari, F., Pleban, T., Perez-Melis, A., Bruedigam, C., Kopka, J., Willmitzer, L., Zamir, D., Fernie, A.R., 2006. Comprehensive metabolic profiling and phenotyping of interspecific introgression lines for tomato improvement. Nat. Biotechnol. 24, 447–454.

Scheideler, M., Schlaich, N.L., Fellenberg, K., Beissbarth, T., Hauser, N.C., Vingron, M., Slusarenko, A.J., Hoheisel, J.D., 2002. Monitoring the switch from housekeeping to pathogen defense metabolism in *Arabidopsis thaliana* using cDNA arrays. J. Biol. Chem. 277, 10555–10561.

Sheveleva, E., Chmara, W., Bohnert, H.J., Jensen, R.G., 1997. Increased salt and drought tolerance by D-ononitol production in transgenic *Nicotiana tabacum* L. Plant Physiol. 115, 1211–1219.

Schneiter, A.A., Miller, J.F., 1981. Description of sunflower growth stages. Crop Sci. 21, 901–903.

Scholes, J.D., Lee, P.J., Horton, P., Lewis, D.H., 1994. Invertase: understanding changes in the photosynthetic and carbohydrate metabolism of barley leaves infected with powdery mildew. New Phytol. 126, 213–222.

Senkoylu, N., Dale, N., 2006. Nutritional evaluation of a high-oil sunflower meal in broiler starter diets. J. Appl. Poult. Res. 15, 40–47.

Sumner, L.W., Mendes, P., Dixon, R.A., 2003. Plant metabolomics: large-scale phytochemistry in the functional genomics era. Phytochemistry 62, 817–836.

Swarbrick, P.J., Schulze-Lefert, P., Scholes, J.D., 2006. Metabolic consequences of susceptibility and resistance in barley leaves challenged with powdery mildew. Plant Cell Environ. 29, 1061–1076.

Tang, X., Frederick, R.D., Zhou, J., Halterman, D.A., Jia, Y., Martin, G.B., 1996. Initiation of plant disease resistance by physical interaction of AvrPto and Pto kinase. Science 274, 260–263.

Tang, S., Yu, J.K., Slabaugh, M.B., Shintani, D.K., Knapp, S.J., 2002. Simple sequence repeat map of the sunflower genome. Theor. Appl. Genet. 105, 1124–1136.

Tavernier, V., Cadiou, S., Pageau, K., Laugé, R., Reisdorf-Cren, M., Langin, T., Masclaux-Daubresse, C., 2007. The plant nitrogen mobilization promoted by *Colletotrichum lindemuthianum* in *Phaseolus* leaves depends on fungus pathogenicity. J. Exp. Bot. 58, 3351–3360.

Tohge, T., Fernie, A.R., 2009. Web-based resources for mass-spectrometry-based metabolomics: a users guide. Phytochemistry 70, 450–456.

Vilo, J., Kapushesky, M., Kemmeren, P., Sarkans, U., Brazma, A., 2003. Expression profiler. In: Parmigiani, G., Garrett, E., Irizarry, R., Zeger, S. (Eds.), The Analysis of Gene Expression Data: Methods and Software. Springer Verlag, New York, NY (p. 5).

Voegele, R.T., Wirsel, S., Möll, U., Lechner, M., Mendgen, K., 2006. Cloning and characterization of a novel invertase from the obligate biotroph *Uromyces fabae* and analysis of expression patterns of host and pathogen invertases in the course of infection. Mol. Plant Microbe Interact. 19, 625–634.

Wagner, C., Sefkow, M., Kopka, J., 2003. Construction and application of a mass spectral and retention time index database generated from plant GC/EI-TOF-MS metabolite profiles. Phytochemistry 62, 887–900.

Zhao, J., Wang, J., An, L., Doergue, R.W., Chen, Z.J., Grau, C.R., Meng, J., Osborn, T.C., 2007. Analysis of gene expression profiles in response to *Sclerotinia*. Planta 227, 13–24.

Zhu, L., Liu, X., Liu, X., Jeannotte, R., Reese, J., Harris, M., Stuart, J., Chen, M., 2007. Hessian fly (Mayetiola destructor) attack causes dramatic shift in carbon/nitrogen metabolism in wheat. Mol. Plant Microbe Interact. 21, 70–78.

Zrenner, R., Salanoubat, M., Willmitzer, L., Sonnewald, U., 1995. Evidence of the crucial role of sucrose synthase for sink strength using transgenic potato plants (*Solanum tuberosum* L.). Plant J. 7, 97–107.

Zucker, M., 1968. Sequential induction of phenylalanine ammonia-lyase and a lyase-inactivating system in potato tuber disks. Plant Physiol. 43, 365–374.

Zulak, K.G., Cornish, A., Daskalchuk, T.E., Deyholos, M.K., Goodenowe, D.B., Gordon, P.M., Klassen, D., Pelcher, L.E., Sensen, C.W., Facchini, P.J., 2007. Gene transcript and metabolite profiling of elicitor-induced opium poppy cell cultures reveals the coordinate regulation of primary and secondary metabolism. Planta 225, 1085–1106.